

SIMPLE AND ROBUST FREE ELECTRON LASER DOUBLER*

S. Di Mitri[†], G. De Ninno¹, R. Fabris, S. Spampinati, Elettra Sincrotrone Trieste, 34149, Italy
 N. R. Thompson², ASTeC, STFC Daresbury Laboratory, Warrington, WA44AD Cheshire, UK
¹also at Laboratory of Quantum Optics, University of Nova Gorica, Nova Gorica 5001, Slovenia
²also at Cockcroft Institute, Sci-Tech Daresbury, Warrington, WA44AD, UK

Abstract

We present the design of a Free-Electron Laser (FEL) doubler suitable for the simultaneous operation of two FEL lines. The doubler relies on the physical selection of two longitudinal portions of an electron bunch at low energy, and on their spatial separation at high energy. Since the two electron beamlets are naturally synchronized, FEL pump-FEL probe experiments are enabled when the two photon pulses are sent to the same experimental station. The proposed solution offers improved flexibility of operation w.r.t. existing two-pulse, two-color FEL schemes, and allows for independent control of the color, timing, intensity and angle of incidence of the radiation pulses at the user end station. Detailed numerical simulations demonstrate its feasibility at the FERMI FEL facility.

INTRODUCTION

We propose a scheme in which two longitudinal portions of the electron bunch (beamlets) are physically selected with a thick mask at low energy in the linac (beam scraping), and spatially separated with a septum magnet at high energy. Each beamlet is then sent to a distinct undulator line. Unlike any of the preceding schemes, ours allows the simultaneous operation of two FEL lines, naturally synchronized at (sub-)fs level, with continuously tuneable relative delay from few fs to ps. Since two undulator lines are used, full and independent control of color, timing, intensity and angle of incidence of the individual radiation pulses on the sample is ensured. If the two FEL pulses are directed to the same user end station, FEL-pump FEL-probe experiments can be done with unprecedented flexibility, either in self-amplified spontaneous emission (SASE) [1,2] or in seeded configurations [3,4].

ELECTRON BEAM MANIPULATION

The scheme is sketched in Fig. 1, and typical parameters at FERMI [5,6] are considered in the following as a case study. A high brightness electron bunch is generated in a photo-injector (gun) and time-compressed in a magnetic chicane (BC1). The bunch length compression factor is $C \equiv \frac{\sigma_{t,i}}{\sigma_{t,f}} \cong \left(1 - \frac{R_{56}\sigma_\delta}{c\sigma_{t,i}}\right)^{-1}$, with $\sigma_\delta = 2\%$ the relative energy spread linearly correlated to the initial bunch duration $\sigma_{t,i} = 2.8$ ps. A mask with two apertures is installed in the middle of BC1, where the particles horizontal position w.r.t. the reference trajectory is $x(s) \cong \eta_x(s)\delta$, and betatron oscillations can be neglected. The mask, made of

~10 mm thick copper, physically selects two transversally displaced beamlets, the rest of the bunch being scattered at large angles and absorbed in the chamber. Since the chicane is achromatic, the two beamlets exit BC1 separated both in energy and in time, but spatially aligned. With V-shape geometry, the vertical position of the mask determines both the width of the two apertures and their transverse separation. The beamlets duration at the exit of BC1, as well as their time separation, is estimated by [7] $\Delta t_{FWHM} \approx \frac{2\Delta x}{\eta_x} \frac{\sigma_{t,i}}{C\sigma_\delta}$, with Δx either the apertures width or the width of the central slit, respectively. For example, with $C = 10$ and $\Delta x = 3$ mm, $\Delta t_{FWHM} \approx 320$ fs.

Downstream of BC1, the linac RF phases are adjusted to ensure both a large relative energy offset of the beamlets (δ_f), which is suitable for their spatial separation in the switchyard, and a small energy spread in each beamlet ($\sigma_{\delta,f}$), as required for efficient lasing. The RF phasing takes into account the effect of the longitudinal wakefields excited by the leading beamlet on the trailing one. For example, we obtain in simulation $\delta_f = 0.9\%$ and $\sigma_{\delta,f} = 0.04\%$. Doing so, the final mean energy is lowered from 1.40 GeV for the standard whole bunch preparation, to 1.25 GeV (see Fig. 2).

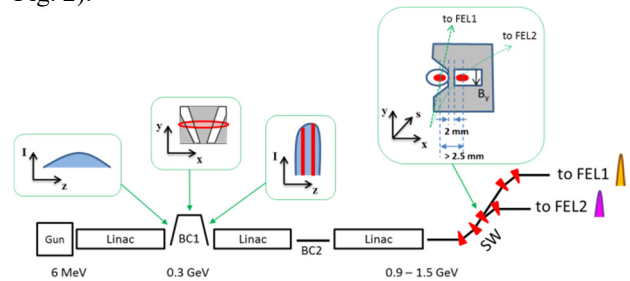


Figure 1: FEL doubler applied to FERMI (not to scale): selection of electron beamlets in BC1 with a mask (red slices), and separation in the switchyard (SW) with a septum magnet.

The FERMI switchyard (SW in Fig. 1) is a ~40 m long line working in the energy range 0.9-1.5 GeV. It comprises two branches, each including two modified double bend achromatic cells. The first cell is in common, and the dipoles bending angle is 3 deg. The two branches lead to the FEL1 and FEL 2 undulator lines; these are parallel and separated by 1 m. Depending on the electron beam energy and on the resonant harmonic jump set by the variable gap undulators, FERMI covers the fundamental wavelength range 20–100 nm with FEL1, and 4–20 nm with FEL2, in high gain harmonic generation (HG) mode of operation [3].

For the purpose of separating the beamlets in the bending plane, the SW optics was modified. A dispersion function

* Work supported by European Union's Horizon2020 research and innovation programme under Grant Agreement No. 777431

[†] simone.dimitri@elettra.eu

as large as -0.3 m is generated at the location of the third dipole magnet, i.e., at the entrance to the FEL2 branch line (see Fig. 1). The dipole magnet would be replaced by a thin septum magnet, having similar length of 0.5 m and the same bending angle. The beamlet at low energy-positive x coordinate is bent by the septum magnetic field and directed to-wards FEL2. The other beamlet continues its straight path towards the next double bend cell, and is eventually directed to FEL1. In order for the two beamlets to safely reach the present common dump at the end of the undulators, the FERMI dump line would be modified. This modification is not required in facilities where multiple dumps downstream of distinct undulators are already available.

Figure 2 shows the beamlets longitudinal phase spaces at the entrance of the septum magnet, for different separations of the apertures in the mask. Particle tracking was carried out with the elegant code [8], including all major collective effects from the injector exit to the undulator. The main beam and mask parameters are listed in Table 1. In this simulation, the outer borders of the mask apertures are kept fixed, so that a larger apertures separation (larger energy offset of the two beamlets) implies a smaller apertures width (shorter beamlets duration). Figure 2 also shows the corresponding horizontal separation of the beamlets at the septum entrance, and their current profile.

Table 1: Electron Beam Parameters at the Entrance of BC1 (Whole Bunch) and of the Undulator (Each Beamlet) as from Tracking Tun. The mask geometry is also reported.

Quantity	@ BC1	@ UND	Units
Charge	0.7	~0.2	nC
Mean energy	0.27	1.25	GeV
Relative energy spread, rms	2.0	< 0.03	%
Duration, fwhm	10.8	0.3	ps
Peak current (core)	650	650	A
Horizontal normalized emittance, projected rms	0.6	0.7	μm
Vertical normalized emittance, projected rms	0.6	0.6	μm
Mask slit width	1		mm
Mask apertures width	3		mm

The horizontal separation of the beamlets at the septum entrance is $\eta_x \delta_f \geq 2.5$ mm, and much larger than their individual betatron beam size. We thus consider a minimum septum thickness of 2 mm, which can be provided by an in-vacuum eddy-current septum magnet. We developed a septum design of 15×25 mm² transversal acceptance. A maximum electric power of ~100 W is expected to be safely dissipated, which translates into a repetition rate of 25 Hz at the beamlets' mean energy of 1.25 GeV. The beamlets' rms position jitter at the septum must be much smaller, say one-tenth, of 2 mm, which implies a relative rms energy jitter of 0.07%, and an overall trajectory jitter ≤ 50 μm . This error budget is well within reach of x-ray FEL facilities [9].

The optics of the switchyard branches is achromatic. Although it is not isochronous ($R_{56} = -0.3$ mm for FEL1, +2.9 mm for FEL2), the beamlets' duration is almost unchanged by virtue of their negligible correlated energy spread, i.e., $\Delta\sigma_t \cong R_{56}\sigma_{\delta,f}/c \leq 4$ fs. The minimum relative delay of the beamlets at the undulator is determined by the difference in the transfer matrix of the two branches: $\Delta t \cong (R_{51}\Delta x + R_{52}\Delta x' + R_{56}\delta)/c \cong (R_{51}\eta_x\delta + R_{52}\eta'_x\delta + R_{56}\delta)/c = (67 + 5 + 75)$ fs = 147 fs in our case.

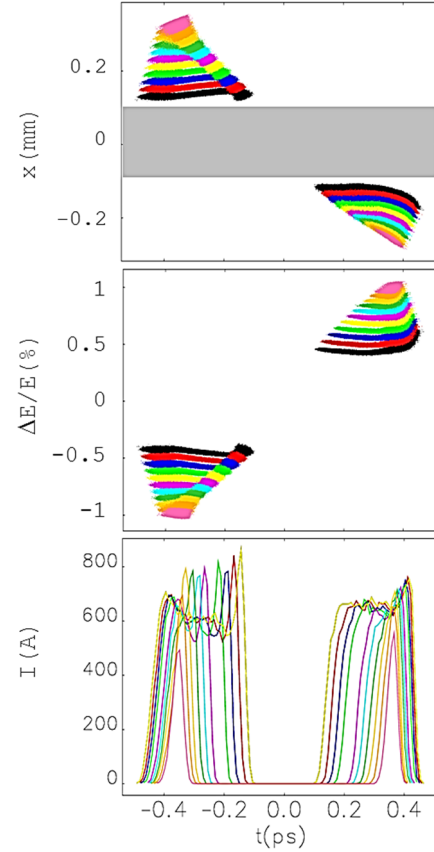


Figure 2: From top to bottom, longitudinal phase space, top view (with shadow of the 2 mm septum thickness) and current profile of the two beamlets at the undulator entrance, for a mask slit width in the range 3–8 mm, and apertures width of 1–6 mm. Bunch head is on the left. The linac RF phases were optimized for one beamlet's duration only (black).

LASING

Figure 3 shows the result of time-dependent FEL1 and FEL2 simulations done with the Genesis 1.3 code [10], for the mask geometry and beam parameters in Table 1. The mask was chosen so as to make the beamlets long enough, approximately 300 fs full width, to accommodate an external seeding laser of 50 fs. The FEL input and output parameters are summarized in Table 2.

We also conducted an experiment with beam and mask parameters close to those in Table 1, but a single mask aperture as due to available hardware. Figure 4 shows the measured spectrum of the first HGHG stage of FERMI

FEL2, tuned at the 8th harmonic of the seed laser wavelength. The seed laser duration was about 50 fs. The spectrum is measured as a function of the delay of the seed laser relative to the electron bunch arrival time. The top plot is without beam scraping; the bottom plot is for scraping in BC1 set to generate beamlet duration of approximately 330 fs. The extension of the lasing region as a function of the seed laser-electron bunch delay confirms the expected beamlet duration, and it highlights a region of efficient lasing in the beamlet as long as ~ 150 fs. The spectrum intensity is normalized to the peak value in both plots: the average FEL pulse energy was 35 μ J for the whole beam, 15 μ J for the selected beamlet without further optimization of the spatial and temporal overlap of seed laser and electron beamlet.

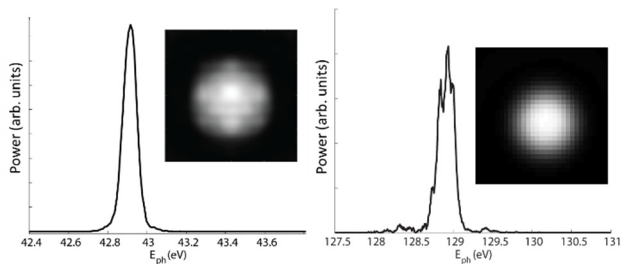


Figure 3: Spectral power and transverse intensity distribution (inset) at the end of the FEL1 (left) and FEL2 undulator line (Genesis 1.3 simulation). Electron beamlets parameters as in Table 1.

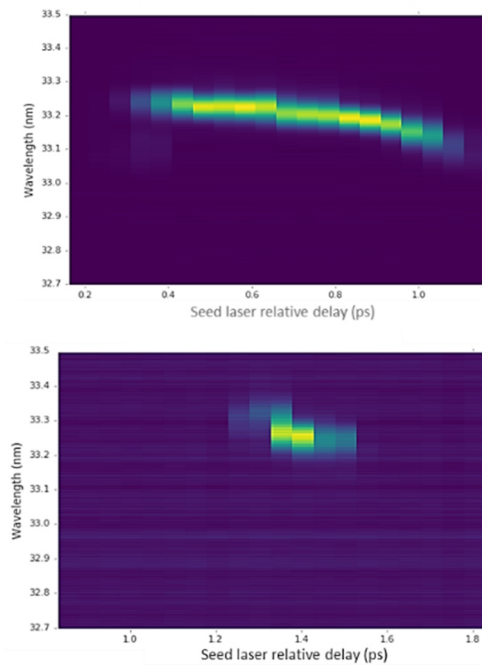


Figure 4: Spectrum of the first stage of FERMI HGHG FEL2 vs. seed laser delay. The seed laser is superimposed to the whole electron beam (top), and to a single beamlet produced with scraping in BC1 (bottom). The spectrum intensity is normalized in both plots to the peak value. The seed is time-shifted in steps of 50 fs, 20 shots are consecutively recorded for each delay value.

Table 2: FEL1 and FEL2 Input and Output Parameters. Electron beamlets parameters as in Table 1.

Quantity	FEL1	FEL2	Units
Seed laser pulse energy	5	10	μ J
Seed laser duration, fwhm	50	50	fs
Harmonic jump	9	27	
Central wavelength	28.8	9.6	nm
Relative bandwidth, fwhm	0.20	0.18	%
Pulse energy	60	13	μ J
Pulse duration, fwhm	30	37	fs
Peak power	2.0	0.4	GW

CONCLUSIONS

In conclusion, we have demonstrated with detailed numerical simulations that two-pulse, two-color FEL emission synchronized at sub-fs level can be generated by splitting the electron bunch in two beamlets, and that these can be safely sent to distinct undulator lines. The scheme is suitable for the simultaneous operation of experimental beamlines receiving FEL pulses generated by very similar *electron* beam parameters, and can be implemented at existing facilities with limited cost and reduced impact on the infrastructure.

Unlike any HGHG option, the proposed scheme has no color limitation due to the harmonic up-conversion of the seed laser wavelength. Accordingly, this study is expected not only to pave the way to simultaneous operation of two synchronized FEL lines, but also to more flexible, robust and reliable two-color, two pulse schemes for, e.g., four wave mixing spectroscopy as well as a broader variety of FEL-pump FEL-probe experiments, including transient grating spectroscopic methods. Since pump and probe are generated with two different undulators, and for relative time separation of the two pulses up to 1 ps or so, there is no need of a large split-and-delay system for the photon beam, which can be costly, difficult to operate, and reducing the photon flux at the sample.

For future facilities with freedom of parameter choice, the two beamlets could be created using a double photo-injector laser pulse, accelerated at the same phase on different RF cycles, before being given small energy offsets in a subharmonic cavity so that they can be separated into two FEL beamlines by the septum with the same scheme presented above. Such double pulse option may offer some more flexibility in beam compression, and avoids relatively large beam power losses induced by scraping at high repetition rates.

REFERENCES

- [1] A.M. Kondratenko and E.L. Saldin, “Generation of coherent radiation by a relativistic electron beam in an undulator”, *Part. Accel.*, vol. 10, pp. 207–216, Aug. 1980.
- [2] R. Bonifacio, C. Pellegrini, and L. Narducci, “Collective instabilities and high-gain regime in a free electron laser”, *Opt. Commun.* vol. 50, pp. 373-378, Jul. 1984.
doi:10.1016/0030-4018(84)90105-6

- [3] L.-H. Yu, "Generation of intense uv radiation by subharmonically seeded single-pass free-electron lasers", *Phys. Rev. A*, vol. 44, pp. 5178–5193, Oct. 1991.
doi:10.1103/PhysRevA.44.5178
- [4] G. Stupakov, "Using the Beam-Echo Effect for Generation of Short-Wavelength Radiation", *Phys. Rev. Lett.*, vol. 102, pp. 074801, Feb. 2009.
doi:10.1103/PhysRevLett.102.074801
- [5] E. Allaria *et al.*, "Highly coherent and stable pulses from the FERMI seeded free-electron laser in the extreme ultraviolet", *Nat. Phot.* vol. 1, pp. 699-704, 2012.
doi:10.1038/nphoton.2012.233
- [6] E. Allaria *et al.*, "Two-stage seeded soft-X-ray free-electron laser", *Nat. Phot.*, vol. 7, pp. 913-918, Oct. 2013.
doi:10.1038/nphoton.2013.277
- [7] W. Qin, Y. Ding, A. A. Lutman, and Y.-C. Chao, "Matching based fresh-slice method for generating two-color x-ray free-electron lasers", *Phys. Rev. Accel. Beams*, vol. 20, pp. 090701, 2017.
doi.org/10.1103/PhysRevAccelBeams.20.090701
- [8] M. Borland, "elegant: A Flexible SDDS-Compliant Code for Accelerator Simulation", Advanced Photon Source Technical Note LS-287, Aug. 2000.
doi:10.2172/761286
- [9] L. Wang *et al.*, "Energy Jitter Minimization at LCLS", in *Proc. FEL'15*, Daejeon, Korea, Aug. 2015, paper TUP070, pp. 523-529.
- [10] S. Reiche, "GENESIS 1.3: a fully 3D time-dependent FEL simulation code", *Nucl. Instrum. Methods Phys. Res., Sect. A*, vol. 429, no. 1-3, pp. 243-248, Jun. 1999.
doi:10.1016/S0168-9002(99)00114-X

Content from this work may be used under the terms of the CC BY 3.0 licence (© 2019). Any distribution of this work must maintain attribution to the author(s), title of the work, publisher, and DOI